IL NUOVO CIMENTO **41 C** (2018) 166
DOI 10.1393/ncc/i2018-18166-8

Colloquia: IWM-EC 2018

New trends in mass identification with telescope detectors

Diego Gruyer(*)
Normandie Univ., ENSICAEN, UNICAEN, CNRS/IN2P3, LPC Caen - F-14000 Caen, France

received 3 December 2018

Summary. — Most open questions in nuclear structure and dynamics require to measure not only the charge but also the mass of reaction products. It is, for example, mandatory in order to constrain the equation of state of asymmetric nuclear matter and its clustering properties at low density, but also to study exotic cluster structures in nuclei. In this contribution, I will report on recent improvements in isotopic identification with telescope detectors. It will cover efforts made by different collaborations around the world to improve detector quality, electronic chains and signal processing. New identification techniques such as Pulse Shape Analysis identification or relative Time-of-Flight identification, as well as their performances, will also be discussed.

1. – Introduction

In the intermediate energy regime, violent heavy-ion collisions produce many nuclear species with a large range of charge (Z), mass (A), and kinetic energy (E). Studying this kind of reactions requires detectors with almost 4π solid-angle coverage, high granularity, low-energy thresholds, large dynamic range in energy and capable of characterizing reaction products on an event by event basis. The first generation of 4π multi-detectors focused on complete collection of charged particles produced in a reaction, providing little isotopic information for heavy fragments ($Z > 5$).

During the first edition of this workshop (2001, Catania, Italy), there has been a round table on "future developments for new generation 4π detectors" and the needs for better isotopic identification was already emphasized by many contributors. In the minutes of the round table [1] we can read : " [...] mass identification over a large solid angle appears as a major necessity for future studies on the role of the isospin degree of freedom with new [radioactive ion beam] facilities. Schematically we can say that the final objective for the next few years would be, if major progresses are obtained, to modify existing multidetectors or to construct a new device at an extra national level."

(*) E-mail: gruyer@lpccaen.in2p3.fr

Indeed, since the first edition of this workshop, detectors have evolved to provide isotopic resolution for a broader range of products, by improving existing detectors and identification techniques, or developing new methods. In this contribution, I will report on recent improvements in isotopic identification with telescope detectors.

2. – ΔE-E identification

The ΔE-E identification method relies on the fact that the stopping power of a material depends on the nature of the incident particle. In fact, for moderate energy particles, the Bethe formula describing the energy loss per distance unit $(-\frac{\mathrm{d}E}{\mathrm{d}x})$ of a particle with charge Z, mass A, and energy E can be roughly approximated as follow:

$$-\frac{\mathrm{d}E}{\mathrm{d}x} \propto \frac{AZ^2}{E}. \tag{1}$$

Figure 1(a) presents for example the energy loss profile of carbon and neon ions with the same incident energy in a given material. The basic idea behind the ΔE-E method is to divide the material into two layers and to measure the energy loss in each of these layers. Such a stacks of detector material layers is called a telescope. The partition of the energy between the two detectors is then different for different particles. The correlation between the energy loss in the first layer versus the total incident energy presented on fig. 1(b) allows to discriminate the Neon from the Carbon. In fact, within this representation, called ΔE-E matrix, different particles populate quasi-parabolic lines characteristic of their charge Z and mass A.

This method is used for many years in nuclear physics and most charged-particle detectors are made of telescopes. Several combinations of detectors have been used for this purpose, such as ionization chambers (IC), silicon detectors (Si), plastic scintillators, or thallium-activated cesium-iodide scintillators (CsI(Tl)). Charge identification can be achieved for many years up to $Z \sim 92$ with various combination of such detectors. Since the mass dependency $(-\frac{\mathrm{d}E}{\mathrm{d}x} \propto A)$ is much weaker than the charge one $(-\frac{\mathrm{d}E}{\mathrm{d}x} \propto Z^2)$, isotopic identification can only be achieved measuring with a very good precision the energy loss in both detector (E and ΔE), while keeping under strict control the thickness of the first layer (Δx).

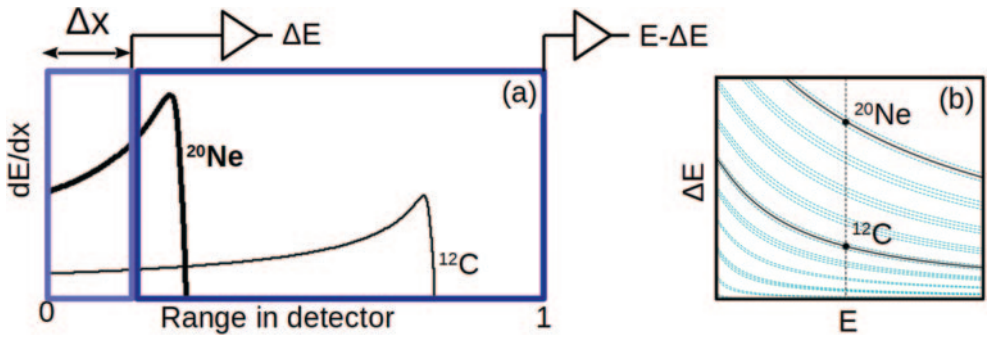

Fig. 1. – Schematic illustration of the ΔE-E method: (a) energy loss profile of neon and carbon ions with the same incident energy in a given material divided in two layers; (b) corresponding ΔE-E matrix.

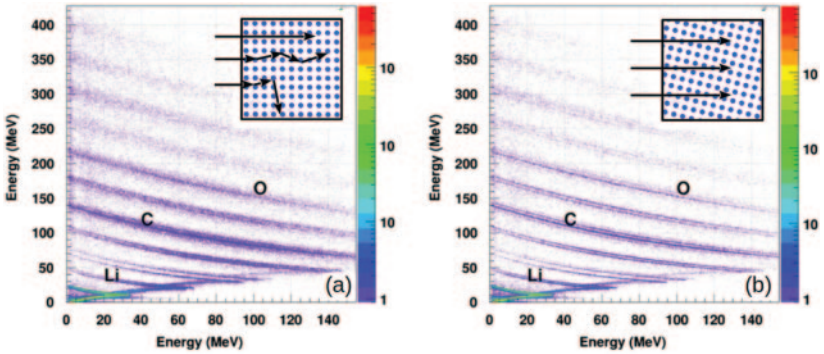

Fig. 2. – ΔE-E identification matrices (Si-Si) for: (a) "channeling" and (b) "random" first silicon crystal orientation (see text). Adapted from [2].

In the following, I will detail two important aspects that have to be considered in order to achieve a good isotopic identification with the ΔE-E method: channeling effects and ΔE detector thickness uniformity.

2˙1. *Channeling effects.* – Crystal-orientation related effects play an important role in pulse-height defect and energy straggling. The signal shape can also be affected by the orientation of the particle ionization track with respect to the crystal planes, thus spoiling the performance of both ΔE-E and PSA identification techniques.

Bardelli and co-workers [3] have shown that, for ions entering the detector along directions parallel to major crystal planes and/or axes ("channeling" configuration), a sizable increase of fluctuations is present with respect to other directions. Impinging directions far from any crystal axis or plane ("random" configuration) correspond to minimal fluctuations in energy and rise-time. Figure 2 presents the ΔE-E correlation obtained from a given tested Si-Si telescopes, both for channeling (a) and random (b) configurations. A clear improvement of the particle identification performance can be easily seen in the random orientation (fig. 2(b)), and in particular an important boost of the isotopic separation.

2˙2. *ΔE detector thickness.* – Manufacturer specification gives usually a thickness uniformity of few μm for silicon detectors. The direct consequence is the impossibility to achieve isotopic identification with large area thin silicon detectors as a first layer. Two solutions can be adopted: 1) not-too-thin silicons (few 100 μm) with a relatively small area (few cm^2) to reduce the relative thickness non-uniformity, or 2) segmented silicons where the thickness can be measured and corrected for each strip or pad.

The first solution has been for example adopted for the FAZIA [4], CHIMERA [5], NIMROD [6] or KRATTA [7] multi-detectors. In the case of FAZIA, the use of 300 μm and 500 μm silicon layers with a $2\times2\,\mathrm{cm}^2$ area ensures a thickness uniformity better than 2%. On the other hand, many detectors such as LASSA [8], HiRA [9], OSCAR [10] or FARCOS [11] use thin segmented detectors. Figure 3 presents the thickness distribution of LASSA and OSCAR stripped silicon detectors. Thickness non-uniformity of OSCAR silicon first layer can reach ∼50% but remains relatively small inside a single strip. In these two cases, correcting for different strip average thickness allows to recover isotopic identification even with such thin detectors.

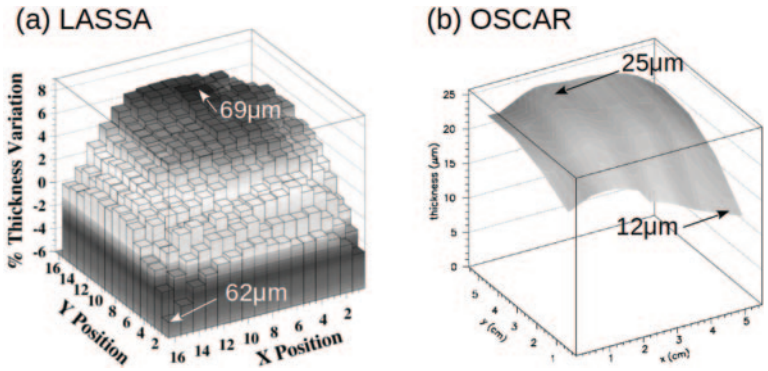

Fig. 3. – 2D map of silicon detector thickness used by: (a) LASSA and (b) OSCAR detectors. Adapted from [8] and [10].

2˙3. *Electronics and signal processing*. – Precise measurement of the energy loss in all telescope layers needs a carefully design of the electronic chain and signal processing. Since very different technologies can fulfill that requirement, I will show here to extreme cases (NIMROD and FAZIA), instead of detailing a specific choice.

The NIMROD super-telescopes [6] are made of two Silicon (Si) layers followed by a CsI(Tl) and uses a fully analogical electronic chain. They allow for isotopic identification up to $Z \sim 14$ in Si-Si matrices and up to $Z \sim 10$ in Si-CsI(Tl) matrices (see fig. 4(a)). On the other hand, FAZIA Si-Si-CsI(Tl) telescopes [12] are readout by a fully digital electronics located as close as possible to the detectors, inside the vacuum chamber. Also in this case, isotopic identification is possible with Si-Si matrices up to $Z \sim 23$ (see fig. 4(b)) and up to $Z \sim 20$ with Si-CsI(Tl) matrices.

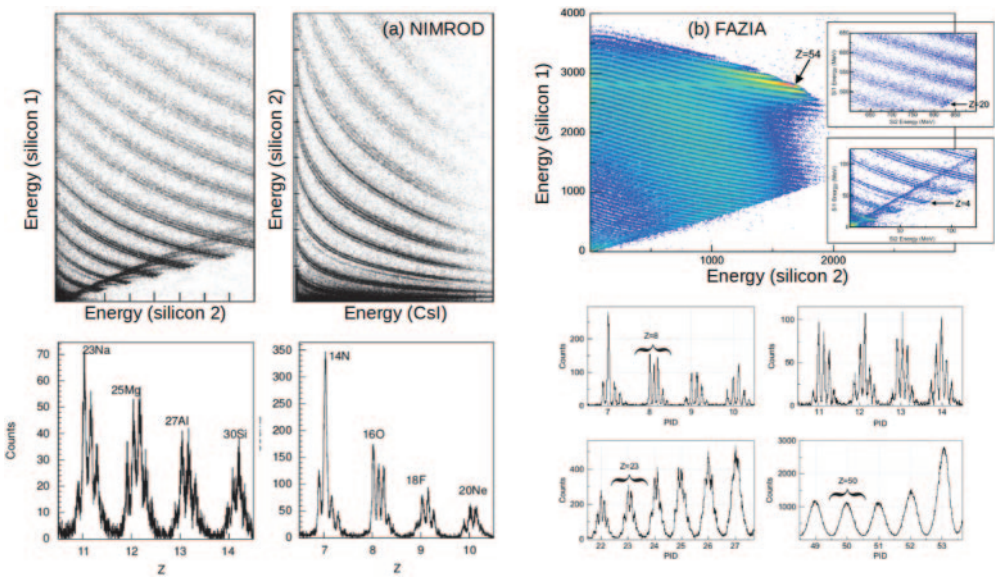

Fig. 4. – Examples of isotopic ΔE-E identification obtained with: (a) NIMROD super-telescopes and (b) FAZIA telescopes. Adapted from [6] and [12].

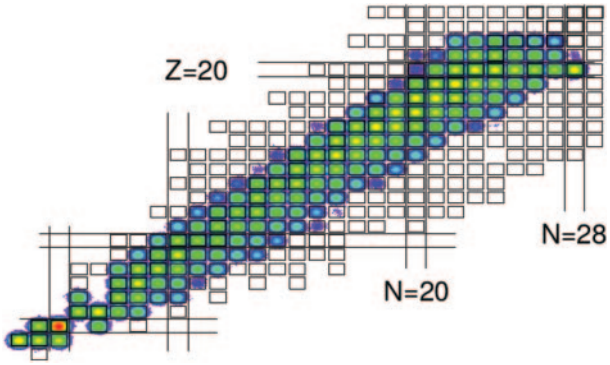

Fig. 5. – Nuclear chart population in ^{48}Ca + ^{48}Ca collisions at 35 MeV/u as seen by the FAZIA detector during the FAZIA-SYM experiment [13].

2˙4. *Performances.* – The ΔE-E identification method, as implemented in modern charged particle multidetectors, is now able to provide isotopic identification up to $Z \sim 20$ for particle crossing the first detector layer (see fig. 5). However it has intrinsic limitations: 1) particles has to cross the first detector and stop in the second, and 2) it allows to identify at most ∼9 isotopes per element. The first limitation can now be overcome thanks to the tremendous improvements in Pulse Shape Analysis identification done in recent years. It is the subject of the next section. The limited number of isotope that can be identified for a given element can be increased by coupling ΔE-E and Time-of-Flight identification. This point will not be treated here but has been discussed in other contributions [14].

3. – Pulse Shape Analysis identification

Because of the different stopping powers described by eq. (1), different particles with the same kinetic energy produce different energy loss profiles along the detector depth (see fig. 6(a)) which results in different charge collection times. The underlying idea of the PSA identification is to use the shape of the signal induced by charge collection to identify particles.

Charge and eventually mass identification with the PSA technique requires a precise measurement of the particle energy and a good characterisation of the signal shape, while keeping under strict control the electric field uniformity and stability.

There are many practical implementations of this technique: using direct or reverse mounted silicon detectors (see fig. 6(a)); extracting information either from charge signal or current signal; and using various algorithms such as fitting procedure [7], analog [5] or digital [15] filtering, or even with artificial neural networks [16]. Finally, PSA allows to use new techniques such as single chip telescopes [7, 17].

3˙1. *Rear and front injection.* – An important aspect to consider when one wants to identify particles using Pulse Shape Analysis in silicon detector is the injection side. Indeed, the signal shape in semiconductors is essentially ruled by two phenomena: the plasma erosion time and the duration of the electron/hole drift towards the appropriate electrode, which strongly depends on the local electric field strength and carrier mobilities.

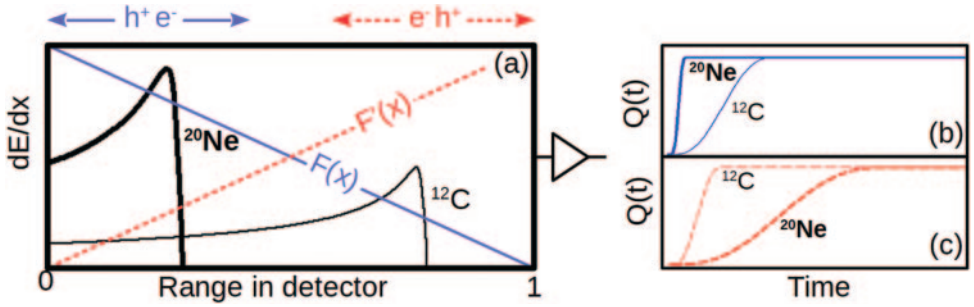

Fig. 6. – Schematic illustration of the Pulse Shape Identification method: (a) energy loss profile of neon and carbon ions with the same incident energy (100 MeV) in silicon material; schematic shape of the signal induced by charge collection for front- (b) and rear- (c) side injection silicon (see text).

In the front-side injection case (particles entering through the high-electric-field side), for particles stopped in the first few microns, the slower charge carriers (the holes) are collected by the close entrance side (front side) and their path lengths are small. Collection times are then short leading to very sharp charge signals (see fig. 6(b)). On the other hand, in the rear-side injection case (particles entering through the low-electric-field side), electrons and holes experience first the low electric field. In particular, the holes which move towards opposite side and have a mobility almost three times lower than the electrons, have to cross a major part of the thickness, thus increasing the collection time. The signals induced by charge collection are much slower than in the case of front side injection (see fig. 6(c)).

Therefore, based on the schematic picture presented in fig. 6, it intuitively appears that rear-side injection will be more favourable for PSA since it shows a larger variety of signal shapes and larger variations of the charge collection time.

In ref. [18], Le Neindre and co-workers (FAZIA collaboration) studied the performances of ΔE-E and PSA identification for rear- and front-side injection silicon mountings. Whereas ΔE-E identification performances are not affected by the injection side, they have shown that the use of reverse mounted silicons (rear-side injection) strongly improves PSA identification capabilities and thresholds. Figure 7 presents the PSA identification matrices using front- (fig. 7(a)) and rear- (fig. 7(b)) side injection silicon detectors. It appears clearly that reverse mounted silicons provide a better identification quality while strongly reducing identification thresholds (fig. 7(c)). Reverse mounted silicon *pin* diodes are also used by the KRATTA array [7]. Slower signals are however less favorable for Time-of-Flight identification.

3˙2. *Electric-field homogeneity and stability.* – The signal shape in semiconductors is strongly affected by the local electric-field strength. Good identification performances can only be obtained using silicon detectors with a high resistivity homogeneity to ensure that particles feel the same electric field strength whatever their impact position on the detector surface (see fig. 8(a)).

In ref. [19], Bardelli and co-workers have developed a PSA-based method that allows for a direct absolute resistivity measurement of the detector as a function of the position with a millimeter resolution. The main advantage of this method is to provide the full resistivity map of a silicon detector in a non-destructive way (see fig. 8(a)). It is then possible to compute the average resistivity non-homogeneity. The FAZIA Collaboration then

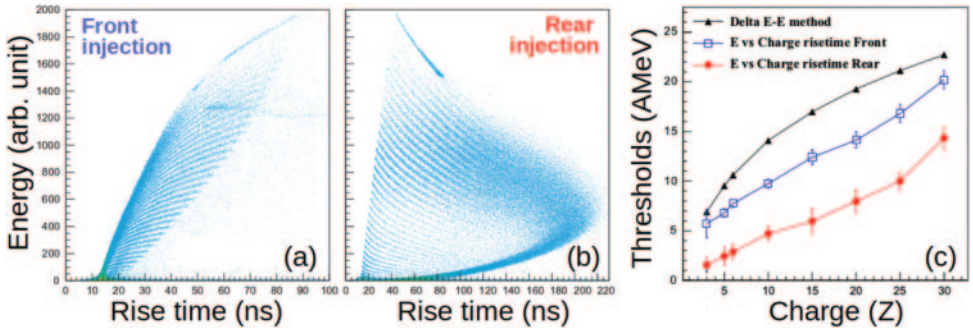

Fig. 7. – Effect of the injection side on Pulse Shape Analysis identification performances: "charge risetime - energy" matrices obtained with (a) front- and (b) rear-side injection silicon semiconductors, and (c) identification thresholds obtained with both configurations. Adapted from [18].

tested PSA performances of silicon detectors with various resistivity non-homogeneity [2] in real experiment conditions. Figures 8(b–c) present examples of PSA matrix obtained with silicon detectors having a ∼5% and ∼1% resistivity homogeneity showing that the identification capability strongly increases with increasing detector homogeneity.

3˙3. *Practical implementation.* – Pulse Shape Analysis identification was first implemented in the CHIMERA mutlidetector. The use of Time-of-Flight Technique (ToF) for mass identification imposes to mount silicon detectors such as particles enter from the high-electric-field side (front-side injection) which is less favorable for PSA identification. Identification is performed using the "charge risetime - energy" correlation made possible by an adaptation of the analogic electronic chain in order to measure two time marks at 30% and 80% of the charge signal. It allows for charge identification of particles stopped in the first telescope layer, being very complementary to the mass identification by ToF measurement.

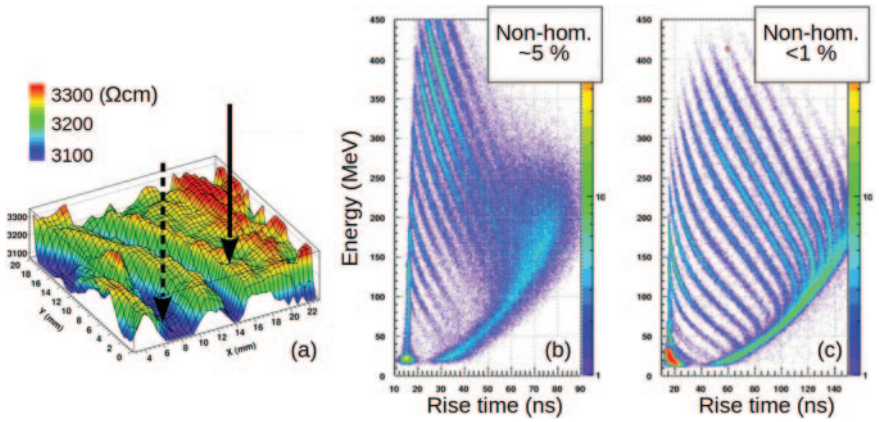

Fig. 8. – Effect of the resistivity homogeneity on Pulse Shape Analysis identification performances: (a) 2D resistivity map of a silicon pad, and "charge risetime - energy" matrices obtained with silicon detectors having (b) ∼5% (c) <1% non-homogeneity. Adapted from [2] and [3].

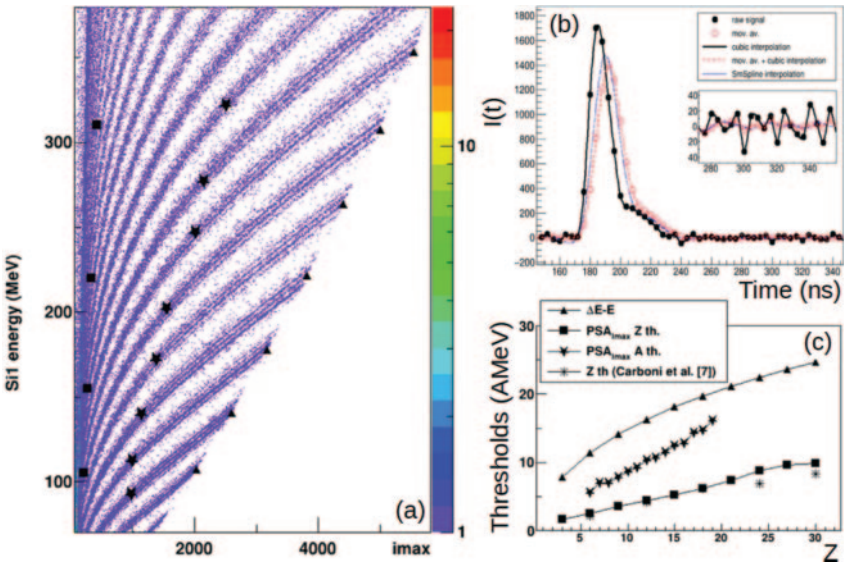

Fig. 9. – Illustration of Pulse Shape Analysis identification as implemented in FAZIA silicon detectors: (a) "current maximum - energy", (b) current signal after various digital filters, (c) identification thresholds. Adapted from [15].

The FAZIA project has been designed in order to optimize PSA identification so it uses reverse mounted silicon detectors (rear side injection). Charge and current signals are digitized as close as possible to the detector in order to preserve their shape so both "charge risetime - energy" and "current maximum - energy" identification can be used. A quantitative comparison of different algorithms conducted by Pastore and co-workers [15] concluded that the best identification performances are obtained using the "current maximum - energy" matrices, after applying a smoothing-spline filter to the current signal digitized at 250 MHz (see fig. 9(b)). Such a matrix is presented in fig. 9(a). It allows for a full charge identification and mass identification up to $Z \sim 20$ with low energy thresholds (see fig. 9(c)).

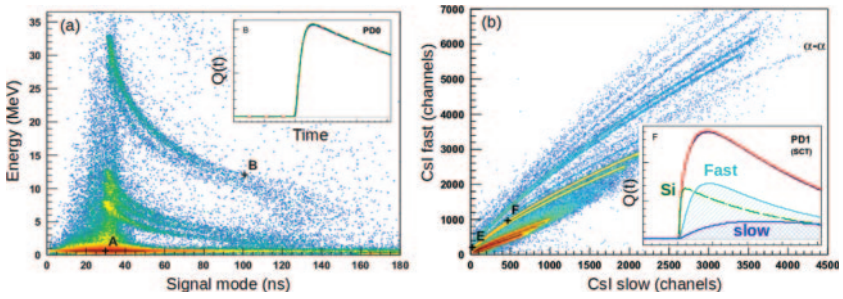

Fig. 10. – Illustration of Pulse Shape Analysis identification as implemented in KRATTA silicon *pin* diodes: (a) "signal mode - energy" matrix obtained by fitting the charge signal of the first *pin* diode (P0) (see inset), (b) CsI(Tl) "fast-slow" matrix obtained after deconvolution of the charge signal of the second *pin* diode (P1) (see inset). Adapted from [7].

The design of the KRATTA [7] array also relies on the use of Pulse Shape Analysis, both to reduce identification thresholds and readout electronics complexity (single chip telescopes). PSA identification in the first *pin* photodiode is performed using the correlation between the particle enegy and the mode of the current signal, extracted by fitting the charge signal (digitized at 100 MHz) with an analytical model. It allows to isotopically identify light charged particles lowering identification threshold to about 2.5 MeV for protons (see fig. 10(a)). PSA allowes also to decompose the complex signals from the middle photodiode into direct ionization and scintillation components (coming from the subsequent CsI(Tl)) and to obtain a satisfactory isotopic resolution, both using Si-CsI(Tl) ΔE-E and CsI(Tl) "fast-slow" matrices (see fig. 10(b)) with a single readout channel. This technique, called "single chip telescope", has also been studied during the FAZIA R&D phase [17] but was not kept in the final design.

4. – Data processing

With increasing numbers of identification matrices to treat which include information on increasing numbers of individual isotopes of different elements, it becomes essential to develop automatic or semi-automatic methods to extract identification lines in ΔE-E or PSA matrices. The need for automation was already evident with the advent of the first large charged particle arrays, and some methods were developed at that time. The evolution of computer resources, and the availability of powerful libraries dedicated to large scale data analysis allow us to consider new types of algorithms. In this section, I will mention three recently proposed algorithms:

- In ref. [20], Lopez and co-workers proposed an improved identification-calibration procedure for Si-CsI(Tl) telescopes, called Advanced Mass Estimate (AME). This procedure, allowing for mass estimation in ΔE-E matrices, relies on an accurate description of the scintillator light response. It has been further extended to identify particles in isotopically resolved FAZIA ΔE-E matrices in a semi-automatic way.

- In ref. [21], Schmidt and co-workers have presented a proof of concept of using an evolutionary strategy to automatically identify particles in ΔE-E matrices. According to the authors, this procedure has been successfully applied to NIMROD Si-Si and Si-CsI(Tl) matrices.

- Finally, ref. [22] presents a semi-automatic method for charge and mass identification, which is based on the identification matrix's properties and uses as little information as possible on the global form of the identification lines, making it applicable to a large variety of matrices (ΔE-E or PSA matrices). Thanks to the implementation in a suitable graphical environment, only two mouse-clicks are required from the user to calculate all initialization parameters. It has been successfully applied to recent data from both INDRA and FAZIA telescopes.

REFERENCES

[1] Borderie B. *et al.*, in *Proceedings IWM2001, LNS-Catania (Italy), November 28 - December 1, 2001.*
[2] Bardelli L. *et al.*, *Nucl. Instrum. Methods A*, **654** (2011) 272.
[3] Bardelli L. *et al.*, *Nucl. Instrum. Methods A*, **605** (2009) 353.

[4] Bougault R. *et al.*, *Eur. Phys. J. A*, **50** (2014) 47.
[5] Pagano A. *et al.*, *Nucl. Phys. A*, **681** (2001) 33.
[6] Wuenschel S. *et al.*, *Nucl. Instrum. Methods A*, **604** (2009) 578.
[7] Lukasik J. *et al.*, *Nucl. Instrum. Methods A*, **709** (2013) 120.
[8] Davin B. *et al.*, *Nucl. Instrum. Methods A*, **473** (2001) 302.
[9] Wallace M.S. *et al.*, *Nucl. Instrum. Methods A*, **583** (2007) 302.
[10] Dell'Aquila D. *et al.*, *Nucl. Instrum. Methods A*, **877** (2018) 227.
[11] Pagano E.V. *et al.*, *Eur. Phys. J. Web of Conf.*, **117** (2016) 10008.
[12] Carboni S. *et al.*, *Nucl. Instrum. Methods A*, **664** (2012) 251.
[13] Camaiani A. *et al.*, these proceedings.
[14] Valdré S. *et al.*, these proceedings.
[15] Pastore G. *et al.*, *Nucl. Instrum. Methods A*, **860** (2017) 42.
[16] Flores J.L. *et al.*, *Nucl. Instrum. Methods A*, **830** (2016) 287.
[17] Pasquali G. *et al.*, *Eur. Phys. J. A*, **48** (2012) 158.
[18] Le Neindre N. *et al.*, *Nucl. Instrum. Methods A*, **701** (2013) 145.
[19] Bardelli L. *et al.*, *Nucl. Instrum. Methods A*, **602** (2009) 501.
[20] Lopez O. *et al.*, *Nucl. Instrum. Methods A*, **884** (2018) 140.
[21] Schmidt K. *et al.*, *JINST*, **12** (2017) P09007.
[22] Gruyer D. *et al.*, *Nucl. Instrum. Methods A*, **847** (2017) 142.